

Cross-Correlation Detection of Point Sources in the WMAP First Year Data *

Jian-Yin Nie¹ and Shuang-Nan Zhang^{1,2}

¹ Department of Physics and Center for Astrophysics, Tsinghua University, Beijing 100084;
science@sina.com

² Key Laboratory of Particle Astrophysics, Institute of High Energy Physics, Chinese Academy of Sciences, Beijing 100049

Received 2006 April 28; accepted 2006 October 18

Abstract We apply a Cross-Correlation (CC) method developed previously for detecting gamma-ray point sources to the WMAP first year data by using the Point-Spread Function of WMAP and obtain a full sky CC coefficient map. We find that the CC method is a powerful tool to examine the WMAP foreground residuals which can be further cleaned accordingly. Evident foreground signals are found in the WMAP foreground cleaned maps and the *Tegmark* cleaned map. In this process 101 point sources are detected, and 26 of them are new sources additional to the originally listed WMAP 208 sources. We estimate the flux of these new sources and verify them by another method. As a result, a revised mask file based on the WMAP first year data is produced by including these new sources.

Key words: cosmic microwave background: WMAP — cross-correlation — radio point source

1 INTRODUCTION

The Wilkinson Microwave Anisotropy Probe (WMAP), as the most precise instrument so far for the full-sky anisotropy in the cosmic microwave background (CMB), has given the best measurements of several key parameters in cosmology (Spergel et al. 2003; Hinshaw et al. 2003; Bennett et al. 2003a). The results of WMAP have been applied in many fields of astronomy with important impact (see, e.g., Tegmark et al. 2004; Nolta et al. 2004). A series of global maps of temperature fluctuations of CMB can be obtained from the WMAP data products. From these maps some useful information can be derived, such as CMB temperature fluctuation power spectra, polarization and so on (Hinshaw et al. 2003; Kogut et al. 2003). These results are crucial for precision cosmology. Most parameters of modern cosmology can be determined by fitting the observed results of CMB with theoretical models (Peiris et al. 2003). Complete subtraction of foreground signals from the original full sky maps is important for reliable estimates of many cosmological parameters (Bennett et al. 2003b). On the other hand, WMAP is so far the only radio observatory covering the whole sky in multi-band from 22.8 GHz (K band) to 93.5 GHz (W band). Searching for radio point sources is another application for these full-sky survey data, which is closely related to foreground subtraction.

In order to subtract foreground signals from WMAP data, the WMAP team has given a list of 208 radio point-sources (205 of them have been cross-identified in other bands and the other 3 point sources have not been identified) (Bennett et al. 2003a, b). The way to generate this list is to apply the filter $b_l / (b_l^2 C_l^{\text{cmb}} + C_l^{\text{noise}})$ on the temperature maps weighted by the square-root of the number of observations, where b_l is the transfer function of the WMAP beam pattern, C_l^{cmb} is the CMB angular power spectrum and C_l^{noise} is

* Supported by the National Natural Science Foundation of China.

the noise power. Then peaks that are greater than 5σ in the filtered maps are fit to a Gaussian profile plus a baseline plane. With this procedure the 208 point source list was made.

In order to search for point sources not in the catalogue released by the WMAP team, we used a cross-correlation (CC) method by cross-correlating the CMB maps and WMAP Point Spread Function (PSF). The calculated cross-correlation coefficients of pixels over the whole sky make up a CC coefficient full-sky map which is then used to search for point sources. At the same time, by carrying out some statistical analysis on this CC full sky map, we can also estimate the foreground residuals of radio point sources in a previously cleaned map, and eventually subtract the uncleaned foreground signals.

2 CROSS-CORRELATION

CC is a common method in data analysis to compare the similarity between two data groups. We use the CC method to analyze the CMB map with the PSF of WMAP. The consistency between the PSF and the data in small local areas in the WMAP sky map can be estimated by this method and can then be regarded as a criterion of the existence of point-sources.

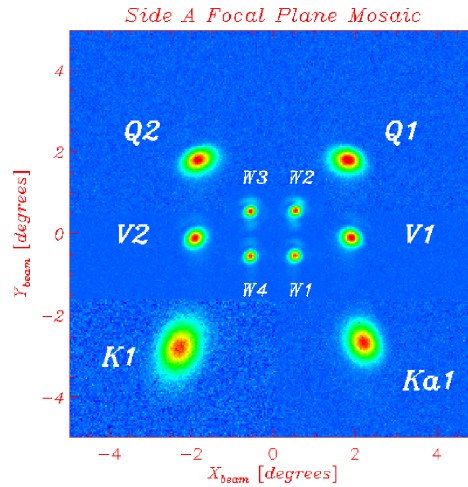


Fig. 1 Beam profile of WMAP in different bands.

Because of the limited angular resolution of WMAP instruments, most radio sources can be considered as ideal point-sources. In the observed WMAP full sky maps, point-sources appear as similar, spread-out two-dimensional Gaussian peaks. In reality, the PSF of each WMAP instrument has its characteristic shape slightly different from an ideal symmetrical Gaussian function. For the convenience of data processing, however, a two-dimensional Gaussian profile is used as the PSF of each WMAP instrument.

We adopt the following equation,

$$C(n) = \frac{1}{m} \sum (D_i - \overline{D})(f_i - \overline{f}), \quad (1)$$

to calculate the CC coefficients, where $C(n)$ is the value of the CC coefficient at point n (Hermsen 1983). This method was developed by the *COSB* team and was applied in *COSB* data analysis by Hermsen (1983) to search for the gamma-ray point sources.

Theoretically, the summation in Equation (1) should be carried out for all pixels in the sky. Actually for pixels far away from the central location of a point source, the effect of the point source is negligible. Therefore, we sum over only m pixels in a small circle of radius about five times of the full-width at half maximum (FWHM) of the PSF around the central point n . Thus, D_i refers to the value of pixel i in this small circular region, $i = 1, 2, \dots, m$, \overline{D} the average of D_i , f_i the value of PSF at pixel i , and \overline{f} the average of f_i , $i = 1, 2, \dots, m$.

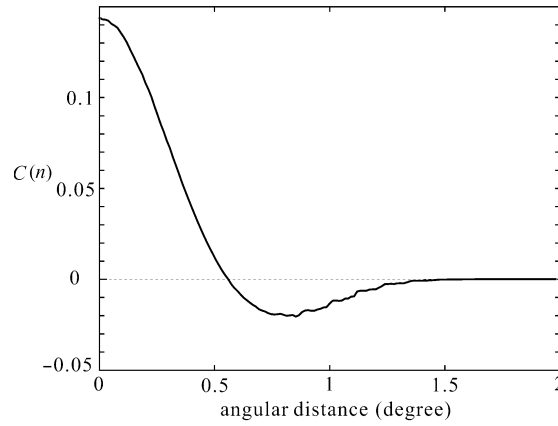


Fig. 2 CC coefficient as a function of the angular distance around an ideal point source for the WMAP Q-band. Note that the CC is negative at about 0.8° – 1.1° , and approaches zero beyond about 1.5° .

Figure 2 shows the CC coefficient distribution around a point source. The figure shows that the CC coefficient has a local maximum value which is directly proportional to the source intensity, if the pixel is just at the location of a point source; for far away pixels the CC coefficient is zero. $C(n)$ can thus be rewritten as

$$C(n) = \frac{A}{m} \sum (f_i - \bar{f})^2, \quad (2)$$

where A is directly proportional to the source intensity. Equation (1) can also be expressed in another form (omitting all subscripts):

$$C(n) = \frac{1}{m^2} \left[m \sum fD - (\sum f)(\sum D) \right]. \quad (3)$$

Since the CMB temperature fluctuations follow a Gaussian distribution, the CC coefficients $C(n)$ also follow a Gaussian distribution in the absence of point sources in the map. Therefore deviations of $C(n)$ distribution from Gaussian are indication of uncleaned point sources in the map. It should also be noted that at certain distances from a given point source, the CC coefficients are negative; therefore, uncleaned point sources can also produce negative deviations from the Gaussian distribution.

3 DATASET

We select three different data sources: the first one is the first year standard data products released by WMAP team published on the website of WMAP mission (<http://lambda.gsfc.nasa.gov>). The foreground cleaned maps, WMAP Internal Linear Combination Map (*ILC* Map) and *imap* data in five bands without subtraction of foreground contamination, are adopted in our work. All these data are organized in the standard format of WAMP data products, with each file involving two one-dimensional arrays, that give the temperature and number of observations of every pixel over the whole sky. The *HEALPix* scheme (<http://healpix.jpl.nasa.gov/>) is adopted to define the position and order of every element in the arrays. In the *HEALPix* scheme, the whole sky is divided into $12 \times N^2$ small patches and every patch has a fixed serial number. For the data we selected, N equals to 512, which means that the whole sky is divided into 3145728 small patches.

The second data source is the *Tegmark* cleaned map (Tegmark et al. 2003) which is considered to be cleaner than the standard WMAP foreground cleaned maps (Liu & Zhang 2005). The *Tegmark* cleaned map is also divided according to *HEALPix* scheme, but contains only one array for the temperature fluctuations.

The third set of data comes from simulations. First, a theoretical power-spectrum is calculated from the basic cosmological parameters published by the WMAP team. The second step is to simulate an ideal

CMB temperature map from this theoretical power-spectrum. Third, smoothing is done using the published WMAP beam profiles. Finally, Gaussian noise of every pixel is added according to the number of observations of every pixel and instrument noise given by WMAP. In this way simulated CMB maps without any point source are produced.

4 DATA PROCESSING

There are strong radio signal contaminations near the galactic equator in the WMAP maps. This kind of strong foreground radio signal cannot be subtracted reasonably cleanly. Therefore, the pixels near the galactic equator cannot be used. To remove those pixels, we applied the Kp2 mask file provided by WMAP, which is one of a series of mask files adopted in WMAP data analysis to subtract the pixels contaminated by galactic equator and strong point sources. The Kp2 mask removes galactic equator and several point sources, retaining about 85% of the original 3145728 pixels. Considering our purpose of surveying for point sources, the Kp2 mask file is divided into the galactic equator and point sources, and we only use the former to remove the pixels near the galactic equator. All of our analyses exclude pixels of the galactic equator.

A new full sky map of CC coefficients can be produced using Equation (1). To further reduce fluctuations due to Gaussian noise and CMB in small scale, a two-dimensional five-point Gaussian smoothing is carried over all pixels. Then possible point sources can be searched by finding local maxima in this map.

To verify the reliability of these point sources and estimate their fluxes, the temperature T at the position of each point source is calculated. For a point source, a series of nested concentric rings 0.1 degree wide are made around the point source and the average temperature within each ring is calculated as a function of the radius. A Gaussian function is used to fit this function and derive the peak value as the temperature of this point source.

5 POINT SOURCE CRITERION

To identify a point source, we introduce the ratio CC/σ_0 , where σ_0 is the parent standard deviation of CC coefficients in a field without any point source. The value of σ_0 is determined from two different datasets. The first one is *imap* data filtered by Kp2 mask. All CC coefficients are grouped according to the number of observations N at every pixel. For each individual group, the distribution of CC coefficients is fitted by a Gaussian distribution and σ_0 of different ranges of N are given. Then the relation between σ_0 and number of observations is fitted by an analytic function, $\sigma_0 = \frac{a}{\sqrt{N}} + b$, as shown in Figure 3.

Another dataset is the simulation data, that contain no point sources and without using the mask. Using the same method, we obtain the coefficients a and b equal to 0.0049 and 0.00145, respectively. Therefore, the difference of σ_0 from these two approaches are less than 5% and in our work we select the σ_0 which

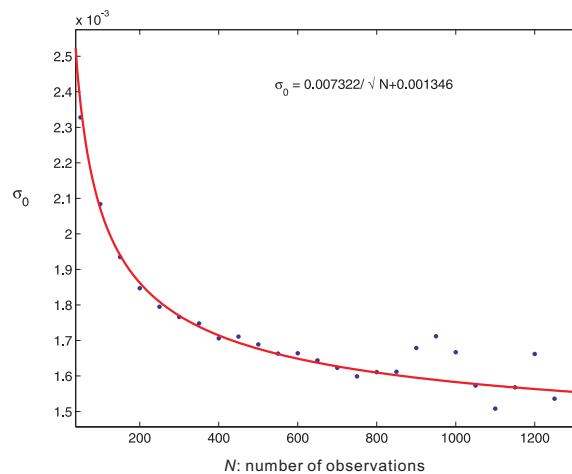


Fig. 3 Relation between number of observations and σ_0 .

comes from true data. From the simulation data, we can also estimate the threshold value of CC/σ_0 ratio for point source detection. In the simulation, we do not find any pixel with CC/σ_0 greater than 5. We therefore choose $5\sigma_0$ as the criterion of point source detection.

6 RESULTS

6.1 Statistical Distribution of CC Coefficients

Figure 4(a)–(d) are the statistical distributions of the CC coefficients of K, Q, V, W band WMAP uncleaned *imap* data and the corresponding simulation data (the X -axis is in units of σ_0). Panels (e) and (f) are the results of WMAP *ILC* map and *Tegmark* cleaned map. From Figure 4(a)–(d) we can find that the distributions of CC coefficients of the simulation data fit Gaussian distribution well. However, the WMAP *imap* data only fit Gaussian distribution well around zero, and there are clear deviations beyond $3\sigma_0$. Even for the *Tegmark* cleaned data shown in Figure 3(f) there are also many pixels with CC coefficients deviated from the Gaussian distribution. Point sources are the natural sources of these non-Gaussian fluctuations, because we have not masked out point sources in calculating these CC coefficients.

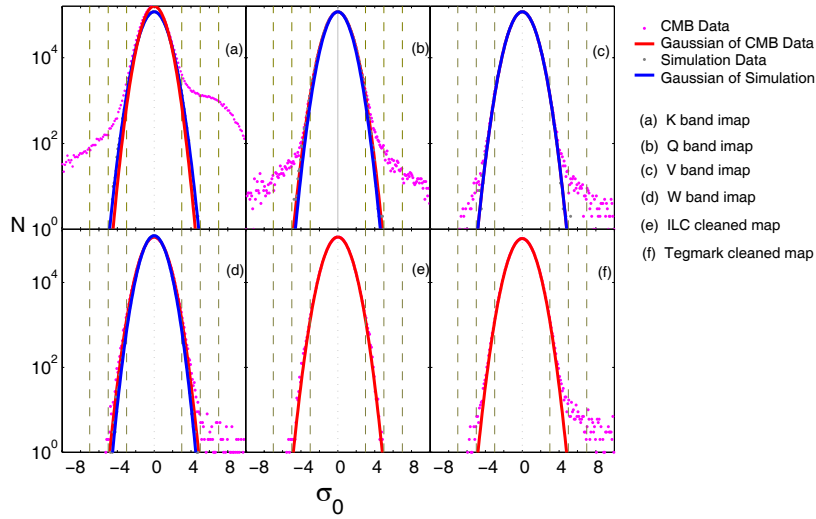


Fig. 4 Statistics of CC coefficient. Purple points are true data and gray points come from simulation. Red and blue lines are the Gaussian fitting results for true and simulation data, respectively. All fitted curves are scaled to the σ_0 and the X -axis is in multiples of σ_0 of the fitted result. Grey vertical dashed lines respectively correspond to ± 3 , ± 5 and $\pm 7\sigma_0$.

For the simulation data, the CC coefficients of all pixels are within the range of $\pm 5\sigma_0$. Because the simulation is a synthesis of the CMB fluctuation and Gaussian noise, we can draw the conclusion that the CMB and the noise cannot make the CC coefficients exceed $\pm 5\sigma_0$. Thus those pixels with CC coefficients beyond $\pm 5\sigma_0$ should be caused by some foreground contamination, which may be point sources. In addition, there are also clear excess of CC coefficient counts between $3\sigma_0$ and $5\sigma_0$. Such coefficients may be caused by other unknown foreground residuals or noise; however, we cannot distinguish between these two possibilities simply from the CC coefficients. Another possibility is that the excess of CC coefficient counts in the range $3\sigma_0$ to $5\sigma_0$ and that beyond $5\sigma_0$ are caused by the same point sources, because several local maxima with different values and at different positions may be produced by one point source.

6.2 Point Source Detection

Applying the local-maxima method to CC coefficients of Q band data, we find 101 local maxima from the pixels with CC coefficients beyond $5\sigma_0$. The comparison between the coordinates of these 101 points and the WMAP published 208 point sources is shown in Figure 5. Obviously these 101 points can be divided

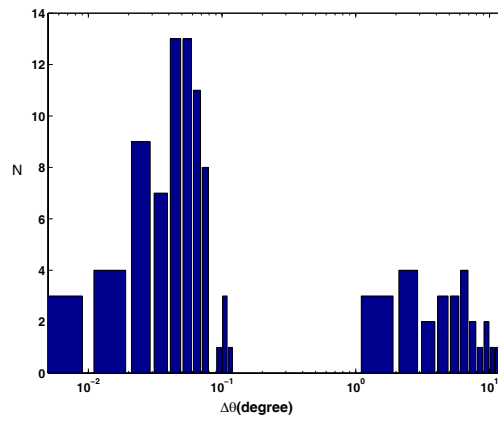


Fig. 5 Histogram of distances of 101 sources detected by local maxima of CC coefficient to the nearest sources in the list of WMAP 208 sources. X -axis is the angular distance and Y -axis the sources count in each distance interval. The 101 points are divided into two groups. The first group shown in the left have distances less than 0.15 degree, therefore the sources detected by CC coefficient and corresponding nearest sources in the 208 source list can be regarded as the same sources. Distances in the other group are all greater than 1 degree. We therefore regard them as new sources which are not in the WMAP 208 source list.

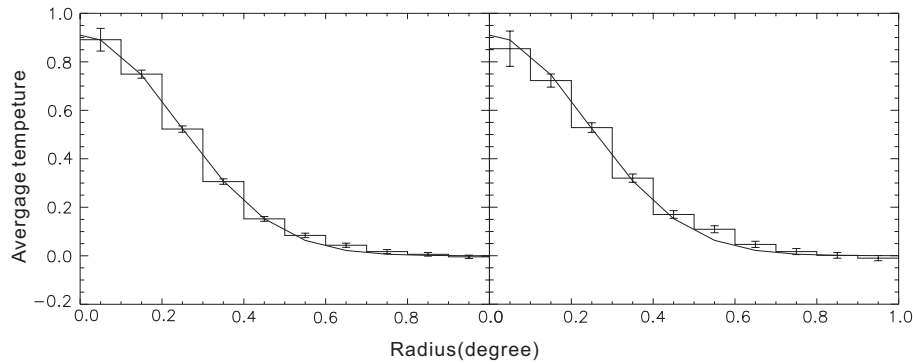


Fig. 6 Consistency of the concentric-ring average temperature and WMAP Q band PSF. In each panel the histogram is the average temperature in different radius from the central points, and the curve is WMAP PSF. The data of all point sources are normalized and then weight-averaged. The left panel shows the average of 15 point sources masked by WMAP Kp2 mask, and the right shows the average of 11 new point sources that are not included in Kp2 mask. The total χ^2 values for the left and right panels are, respectively, 14.2 and 18.0 for 9 degrees of freedom.

into two groups. One group has 75 points, which have distances to the nearest point sources in WMAP list less than 0.15 degree. The distances of 26 points in the other group are all greater than 1 degree. Taking into account of the angular resolution of WMAP in Q band, we regard that the 75 points in the first group to be the same as the corresponding sources in the WMAP 208 point sources. The 26 points of the second group are considered as possible new point sources not included in the WMAP list.

We also compare the locations of our 26 new point sources with WMAP Kp2 mask files of both the first and three year data releases; 15 of our 26 new sources are included in both Kp2 masks and other 11 point sources are missed in the Kp2 mask. In Figure 6 we plot the average temperature at different radius around the location of these 26 points and find that the temperature distribution fits the WMAP Q band PSF well, indicating these sources are consistent with the point sources within the angular resolution of the WMAP Q

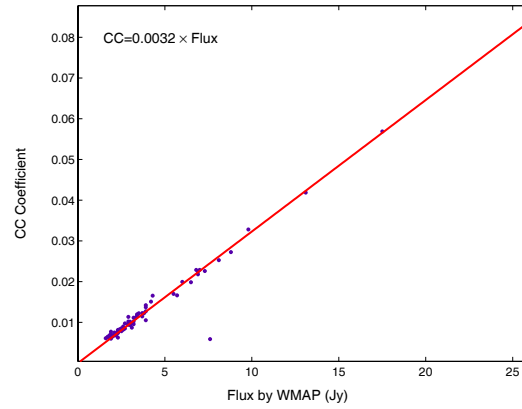


Fig. 7 Linearity of the CC coefficient and Q band intensity given by WMAP, for the 75 sources in the first group shown in Fig. 5.

Table 1 Position and Intensity of 26 New Sources

	l [$^{\circ}$]	b [$^{\circ}$]	CC	Flux [Jy]	Masked by Kp2 mask
1	302.0	-45.0	0.0074	2.3	N
2	303.3	-43.9	0.0068	2.1	N
3	277.3	-36.1	0.0133	4.2	Y
4	280.8	-35.5	0.0070	2.2	N
5	254.9	-33.8	0.0065	2.0	Y
6	278.3	-33.3	0.0060	1.9	Y
7	280.3	-33.3	0.0060	1.9	Y
8	277.6	-32.3	0.0062	1.9	N
9	281.9	-32.1	0.0059	1.8	N
10	279.5	-31.7	0.1117	34.9	Y
11	187.5	-20.7	0.0079	2.5	Y
12	9.3	-19.6	0.0391	12.2	Y
13	263.1	-16.7	0.0063	2.0	Y
14	213.7	-12.6	0.0250	7.8	Y
15	72.7	-9.4	0.0067	2.1	N
16	75.5	-8.8	0.0062	1.9	N
17	227.7	-7.8	0.0067	2.1	N
18	224.4	2.5	0.0063	2.0	N
19	227.7	3.1	0.0112	3.5	Y
20	278.0	4.3	0.0066	2.1	N
21	318.2	10.9	0.0061	1.9	Y
22	327.6	14.6	0.0062	1.9	N
23	34.9	17.6	0.0121	3.8	Y
24	308.8	17.9	0.0104	3.3	Y
25	309.6	19.4	0.1197	37.4	Y
26	21.2	19.6	0.0103	3.2	Y

Note: The error of the CC coefficient is about 0.0012, corresponding to the error of point source flux of approximately 0.4 Jy.

band beam. To eliminate the contamination of these missed point sources, a new mask file including these 11 missed point sources is necessary.

As mentioned above, the CC coefficient $C(n)$ at the center of a point source is proportional to the intensity of this point source. For the 75 point sources of the first group, the CC coefficients and the Q band intensity determined by the WMAP team are correlated in Figure 7. As expected, a good linearity is present. The intensity of the other 26 sources of the second group can be estimated by this linear relation. The coordinates and Q band intensity of these 26 new point sources are listed in Table 1.

6.3 Consistency Check of These Point Sources

Using the concentric-ring-averaging method described in Section 4, the temperatures of all WMAP 208 sources are calculated and correlated with their intensity in Q band determined by the WMAP team. See Figure 8. A good linearity is clearly seen (there are only 185 sources in this figure because intensities of 23 sources were not given in WMAP source list). There is one point significantly far away from the fitted line, which was excluded in the linear fitting. The reason for this deviation will be explained later. Applying this linear function to the 101 point sources found with local maxima of CC coefficients, their intensities can be derived from their temperatures determined in the same way. Another set of intensity of these 101 point sources are also obtained from the CC coefficient by the linearity shown in Figure 7. Figure 9 shows the linear correlation between these two sets of source intensities, indicating consistency of the two methods and thus reliability of the 101 point sources detected in this work.

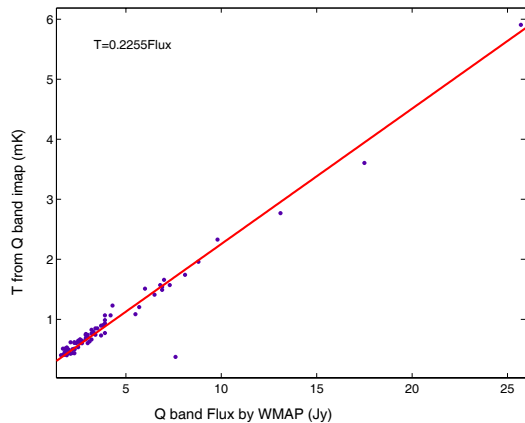


Fig. 8 Linearity of correlation between Q band flux and temperature at the corresponding positions in the WMAP sky map.

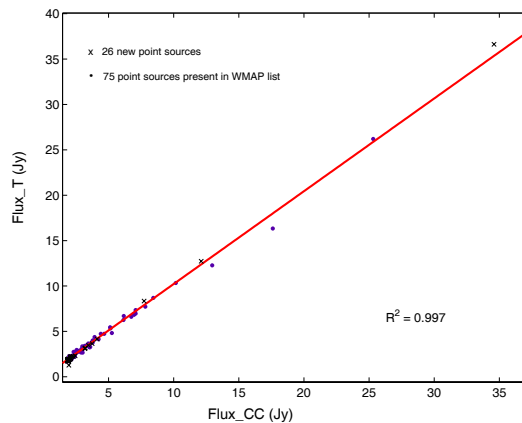


Fig. 9 Linearity of correlation between the two sets of flux derived from two different ways for the 101 point sources. The X -axis is the flux derived from local maxima of CC coefficients and Y -axis is the flux derived from the temperatures at the corresponding position in the all-sky map.

From the linear relation of CC coefficient and source intensity, the intensity threshold corresponding to the $5\sigma_0$ detection threshold of the CC coefficient, is about 1.9 Jy. Comparing with the WMAP 208 source list, about 50 percent of sources with intensity 1.8–2.0 Jy in WMAP source list are detected by us; this agrees with theoretical expectation for the instrumental detection sensitivity (Zhang & Ramsden 1990). For the other 61 sources with intensities greater than 2 Jy in WMAP list, only two are not detected by our method.

For these two undetected sources with intensity greater than 2 Jy, their intensity values are 2.2 ± 0.3 and 2.4 ± 0.4 Jy, respectively. It is reasonable that these sources were not detected because of the uncertainties of their intensity. It is noticeable that in Figure 8, there is one point obviously deviating from the fitting line, which is the point with intensity of 7.6 ± 3 Jy in the WMAP list. According to the CC coefficient at the source location, the estimated intensity is only about 1.8 Jy. As a matter of fact the intensity of this source has been revised to 0 Jy in the new WMAP three year result, which is in good agreement with our result (0 means that the detection significance for this point source is weak, i.e., with intensity less than 2σ in this band).

The consistency of these two methods verifies the reliability of the CC method in point source detection. Although there is a need for improvement of the detection threshold limit, applying this method to data of other WMAP bands should allow more point sources to be detected. A new catalog of point sources based on multi-band WMAP full sky survey is expected in our further work.

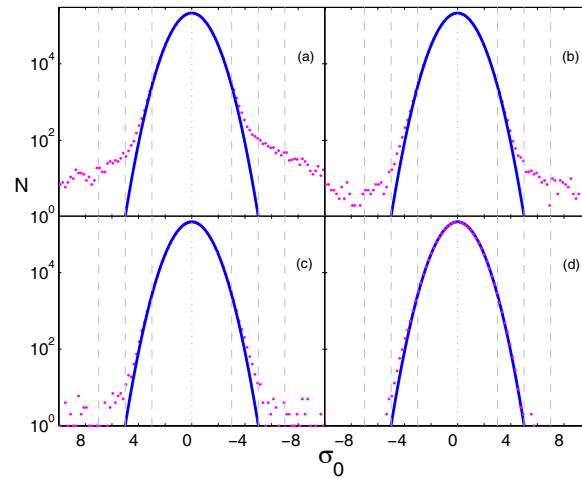


Fig. 10 Statistics of CC coefficient using different foreground subtraction method. X -axis is in multiples of σ_0 , and the gray vertical lines indicate ± 3 , ± 5 and $\pm 7\sigma_0$, respectively. The dots are actual data and the solid lines are the fitted results. Different subtractions of point sources are used. (a) Full foreground cleaned WMAP map (the corresponding *Tegmark* map result is in Fig. 4(f)) without any point sources subtraction; (b) WMAP 208 sources subtracted; (c) full Kp2 mask subtracted; (d) WMAP Kp2 mask, WMAP 208 sources and our 26 new point sources subtracted.

6.4 Revised Mask File

The distribution of CC coefficients for an ideal CMB (with Gaussian noise) map must be a Gaussian distribution, and foreground contamination may cause deviations from the Gaussian distribution. Therefore, CC coefficient provides a powerful tool to check the effectiveness of the foreground subtraction. The WMAP foreground cleaned map (Fig. 10(a)) and the *Tegmark* cleaned map (Fig. 4(f)) are analyzed using CC coefficient, and it was found that both maps contain a lot of signals possibly from point sources. Figure 10(b) shows the CC coefficient distribution after excluding the WMAP 208 point sources, showing obvious deviations from the Gaussian curve, suggesting the existence of more point sources. Many point-sources or point-like sources, which include 182 point-sources in the WMAP 208 source list and 15 sources of our 26 new point sources, are removed by using the Kp2 mask. Applying the full Kp2 mask on Q band cleaned map, Figure 10(c) is obtained, which is much cleaner but still with some pixels exceeding $\pm 5\sigma_0$. Then Figure 10(d) is produced by subtracting from Figure 10(c) *all* 26 new sources detected in this work and *all* WMAP 208 sources; in this case the distribution of CC coefficients fits the Gaussian distribution well. This is the most cleaned map among these four maps and is the least contaminated one by point sources.

We have discussed that around a point source, negative CC coefficients such as that shown in Figure 4(a)–(d) and Figure 10(a)–(c) can arise, as shown in Figure 2. However, after all point sources are subtracted from Q band *imap* data, and convolving with the PSF for the determined intensities, we found that most pixels with negative CC coefficient less than $-5\sigma_0$ no longer appear. See Figure 10(d).

According to the above results, a revised mask file was made. This new mask file includes the full WMAP Kp2 mask, 26 point sources in the WMAP 208 source list that were left out in the Kp2 mask file, and also 11 new point sources (of the 26 new pointed sources detected in our work) not included in the Kp2 mask file. Using this revised mask file in data analysis, we can achieve a cleaner full sky map than the original Kp2 mask.

6.5 Comparison with the WMAP Three Year Products

The WMAP team released their three year data products on Mar 16, 2006 (Hinshaw et al. 2006). In the three year data products, the point source list is expanded to 373 sources (including first year 208 point sources). The expansion of WMAP source list is a result of higher signal-to-noise ratio owing to a greater number of

observations. In the first year WMAP result, the threshold of detection of point sources is about 2.0 Jy in all bands. More observation time will bring a lower threshold. So most additional point sources in WMAP new 373 source list are weaker than 2.0 Jy. Only one new point source of our 26 new sources is included in WMAP newest point-source list because most our new 26 sources are brighter than 1.9–2.0 Jy, which does not overlap the flux range of these additional point sources in WMAP three year list.

7 SUMMARY AND DISCUSSION

We have presented some applications of the CC method in WMAP data analysis, then verified the effectiveness and reliability of this method. Departures of the CC coefficient distribution from the Gaussian distribution imply the existence of point sources in the map. We have searched for local maxima of the CC coefficients from pixels with CC coefficients above $5\sigma_0$ as candidate point sources from WMAP Q band data; a total of 101 sources are detected and 26 of that are new point sources, i.e., have not been detected previously in WMAP band. Comparing with only 61 point sources detected by WMAP in Q band, our method is more sensitive in point source detection. The intensities of these point sources are also compared with results derived from other method, and their mutual consistency is confirmed. According to the result of simulation, the CC method could only detect point sources in pixels beyond $5\sigma_0$, corresponding to a flux density threshold about 1.9 Jy, due to the combined effects of CMB fluctuations and WMAP antenna noise.

The CC coefficient can also be used to examine the foreground contamination of a sky map. Using the CC coefficient, we found there are still some point sources remaining in the WMAP foreground cleaned maps and *Tegmark* cleaned map. A revised Kp2 mask file is made, by including the original WMAP 208 and our new 26 point sources. The distribution of CC coefficients fits the Gaussian curve well for the new map after removing those contaminated pixels using this new mask file.

Our results indicate that the CC method is effective and accurate in point source detection in WMAP data. Our next step is to apply this method to WMAP data in all bands including the three year data. We anticipate more point sources will be detected, thus producing eventually a cleaner foreground-free sky map.

Acknowledgements The authors thank Professor T. P. Li, for kind comments and suggestions, which helped us to improve the method of data processing. We are very grateful to the anonymous referee whose detailed and insightful comments and suggestions allowed us to clarify several issues and improve the readability of this paper. We acknowledge the use of the LAMBDA. Supports for LAMBDA is from the NASA Office of Space Science. This work has used the software package HEALPix (hierarchical, equal area and iso-latitude pixelization of the sphere, <http://www.eso.org/science/healpix>), developed by K.M. Goshen et al. This research has made use of the Astrophysical Integrated Research Environment (AIRE) which is operated by the Center for Astrophysics, Tsinghua University. SNZ acknowledges partial funding support by the Ministry of Education of China, Directional Research Project of the Chinese Academy of Sciences under project No. KJ CX2-YW-T03, and by the National Natural Science Foundation of China (NSFC) under project No. 10521001.

References

- Bennett C. L., Halpern M., Hinshaw G. et al., 2003, ApJS, 148, 1
- Bennett C. L., Hill R. S., Hinshaw G. et al., 2003, ApJS, 148, 97
- Hermesen W., 1983, SSRv, 36, 61
- Hinshaw G., Spergel D. N., Verde L. et al., 2003, ApJS, 148, 135
- Hinshaw G., Nolte M. R., Bennett C. L. et al., 2006, astro-ph/0603451
- Lin X., Zhang S. N., 2005, ApJ, 633, 542
- Kogut A., Spergel D. N., Barnes C. et al., 2003, ApJS, 148, 161
- Nolte M. R., Wright E. L., Page L. et al., 2004, ApJ, 608, 10
- Peiris H. V., Komatsu E., Verde L. et al., 2003, ApJS, 148, 213
- Spergel D. N., Verde L., Peiris H. V. et al., 2003, ApJS, 148, 175
- Tegmark M., Strauss M. A., Blanton M. R. et al., 2004, PhRvD, 69, 103501
- Tegmark M., de Oliveira-Costa A., Hamilton Andrew J. et al., 2003, PhRvD, 68, 123523
- Zhang S. N., Ramsden D., 1990, ExA, 1, 145